CIRCULATION IN THE SKAGERRAK/NORTHERN NORTH SEA: INSIGHT INTO LOCAL RESPONSE (EDDIES) TO LARGE SCALE FORCING USING A NUMERICAL MODEL

LARS PETTER RØED[1,2], JON ALBRETSEN[1], AND INGERID FOSSUM[1]

[1]Norwegian Meteorological Institute, Oslo, Norway
[2]Institute of Geosciences, University of Oslo, Norway

Abstract

We assess the performance of a marginally eddy-resolving numerical ocean model in simulating the circulation and hydrography in the Skagerrak/northern North Sea area. We aim at explaining why recurrent anticyclonic eddies observed in the area off the southern tip of Norway appears. Since these structures result from highly non-linear processes, we have to resort to a numeric ocean model to explain them. The model we use is MI-POM, a version of the widely used Princeton Ocean Model (POM). To resolve the eddies we emply a mesh size of 4km for a limited region (the Skagerrak/northern North Sea area) nested into a coarser grid covering a larger geographical domain. A series of experiments are conducted simulating the eddy response for various years which differ in the representations of the lateral freshwater supply to the nested system. The atmospheric input is extracted from the ECMWF's ERA40 reanalysis data and is in turn used to compute all necessary dynamic and thermodynamic forcing. For validation a comparison against *in situ* hydrographic data is performed. To analyze the nonlinear behavior of the model we employ a recently developed energy diagnostic scheme combined with a potential vorticity analysis.

We find that in general the model faithfully reproduces many of the observed hydrographic structures including their mean patterns and their variance. We also find that the Baltic outflow is by far the most significant freshwater source in terms of its influence on the hydrography in the area. Despite this fact realistic representation of the freshwater is of minor importance regarding frontogenesis and cyclogenesis. Maxima in energy conversions, rooted in strong barotropic and weaker baroclinic instabilities, are found east of the recurring eddy region. Very few signs of instabilities are observed in the eddy region itself. This indicates that the origin of the eddies is upstream of the eddy region, and that barotropic instabilities dominates the cyclogenesis process. Most instabilities are present in the autumn and winter and is found to be associated with outbreak events of low salinity water from the Skagerrak. We also find that the observed persistent enhanced variability off the northwest coast of Denmark is associated with an energy conversion rooted in sea level variations rather than instabilities. Finally we remark that further exploration of the impact of the lateral open boundary forcing, e.g., the input of Atlantic water, is needed.

1. INTRODUCTION

The large scale circulation in Skagerrak is generally cyclonic. Warm and saline Atlantic water masses flow from the west toward the northeastern coast of Denmark where it mixes with less saline water first from the southerpart of the North Sea and later with water masses of Baltic origin. It then first continues along the Swedish coast before it turns west and southwards out along the southeastern coast of Norway as the Norwegian Coastal Current (NCC) (*Svansson*, 1975; *Rodhe*, 1987; *Danielssen et al.*, 1997). The main characteristic of the NCC is its high temporal and spatial variability. One of the areas where the variability is most pronounced, is the area off the southern tip of Norway where the NCC turns northward (*Sætre and Mork*, 1981). This is also known to be an area of high biological production (*Skogen et al.*, 2002, 2003). Thus to understand the oceanic biological production, it is important to be able to forecast such mesoscale variability. Another area of high variability is northwest of Denmark. Generally thses areas of high variability is known among sailors to be difficult and hazardous waters to navigate, a further motivation for being able to forecast them with some certainty.

We present here results from studies performed by *Røed and Fossum* (2004), *Albretsen and Røed* (2006a), *Fossum* (2006), *Røed* (2006), *Albretsen and Røed* (2006b), and *Albretsen* (2006) relating to these mesoscale features. The aim is to explain why recurrent anticyclonic eddies observed in the area off the southern tip of Norway appears, and possibly enhance our ability to forecast them. Since mesoscale structures and their development are highly non-linear features we make use of a numerical model as outlined in Section 2.

The analysis method we use is novel and was developed recently by *Røed* (2006) inspired by a similar study for a layered model by *Røed* (1999). This was simplified by *Fossum and Røed* (2006) who then employed it combined with a potential vorticity (PV) analysis tool to study instabilities in an idealized setting. Later it was used both by *Fossum* (2006) and *Albretsen* (2006) for investigating mesoscale sturctures in the Skagerrak/northern North Sea area. The PV analysis is based on the work of *Charney and Stern* (1962). These analysis tools are used to analyze model results from year long simulations, thus enabling us to study the seasonal variation of the instabilities.

2. MODEL OCEAN

The ocean model we employ is MI-POM, the Norwegian Meteorological Institute's version of the terrain-following (σ-coordinate) Princeton Ocean Model (*Røed and Fossum*, 2004; *LaCasce and Engedahl*, 2005, and references therein). We employ exactly the same doubly nested model system as reported in *Røed and Fossum* (2004), and *Albretsen and Røed* (2006a). For further details on the model and the model set up the reader is therefore referred to the above references. Note that the fine mesh model has a mesh size of 4 km, while the coarser mesh model employs a mesh size of 20 km. The geographical coverage is displayed in Figure 1.

The governing equations are the common conservation equations for mass, momentum, thermal energy and salinity combined with a non-linear equation of state relating density to temperature, salinity and pressure. Also the hydrostatic and Boussinesq approximations are employed. These partial differential equations possess two prominent

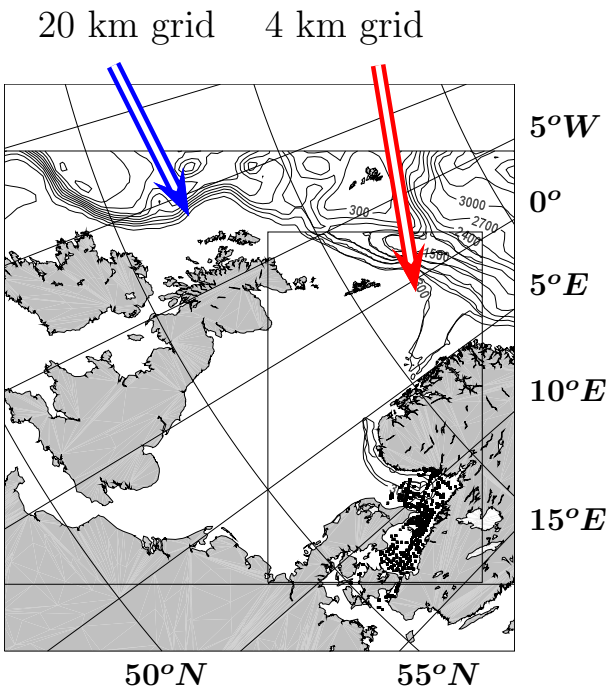

FIGURE 1. Map of the computational domain and the location where validation data are available. Large quadratic area corresponds to the coarse mesh (20 km grid) model, while the smaller rectangular area depicts the fine mesh Skagerrak/northern North Sea area (4 km grid). Heavy black curves indicate bottom topography (300 m contour interval). Locations where validation data for 1998 are available are marked by black dots.

first integrals, namely energy and potential vorticity. The equations are then solved on a computer using finite difference techniques.

3. ANALYSIS METHODS

3.1. **Energy diagnostics.** An energy equation is first derived from the governing equations. The energy is then separated into its kinetic and potential parts as described in *Røed* (1999), and then further split into its mean and eddy components. Since we only want to distinguish barotropic from baroclinic instabilities, a separation into a mean and an eddy part is only necessary for the kinetic energy. Thus we are left with three energy equations, namely

$$\partial_t K_M + \nabla_\sigma \cdot (\mathbf{F}_{K_M} + \mathbf{F}_R) = C_M^\Phi + C_{ME} + S_{K_M}, \quad (1)$$

$$\partial_t \overline{\Phi} + \nabla_\sigma \cdot (\overline{\mathbf{F}}_\Phi + \overline{\mathbf{P}}) = -C_M^\Phi + C_E^\Phi + S_\Phi, \quad (2)$$

$$\partial_t K_E + \nabla_\sigma \cdot \mathbf{F}_{K_E} = C_E^\Phi - C_{ME} + S_{K_E}. \quad (3)$$

where ∇_σ represents the horizontal del operator in σ-coordinates. The pointwise (in the horizontal) depth integrated mean and eddy kinetic energy components are denoted K_M

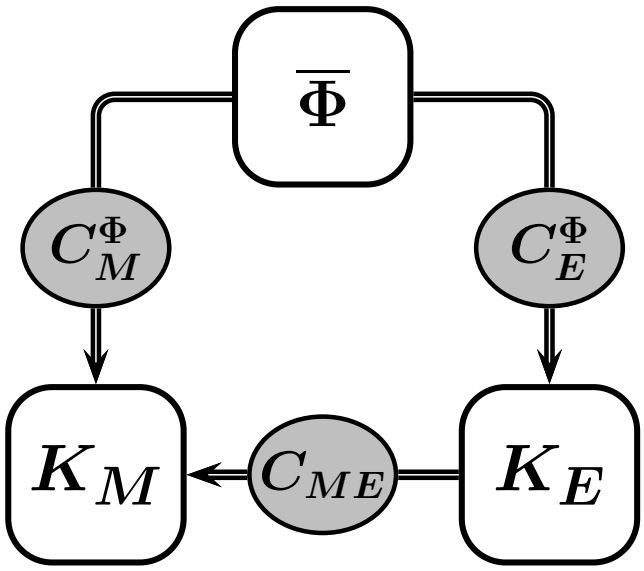

FIGURE 2. Reversible energy transfer routes in the employed energy diagnostic scheme. K_M and K_E are respectively the mean and eddy kinetic energy compartments, while $\overline{\Phi}$ is the average potential energy compartment. The two conversion terms C_{ME} and C_E^Φ may increase the eddy kinetic energy. The direction of the arrow indicates in which direction transfer takes place when the conversion term in question is positive.

and K_E, respectively, while average potential energy is denoted $\overline{\Phi}$. $\mathbf{F}_{K_M}$, $\mathbf{F}_{K_E}$, $\overline{\mathbf{F}}_\Phi$ and $\overline{\mathbf{P}}$ denote the fluxes of mean kinetic energy, eddy kinetic energy, average potential energy and the average pressure flux, respectively, while $\mathbf{F}_R$ is the flux of eddy stress by the mean flow. The terms S_{K_M}, S_{K_E} and S_Φ represent the irreversible loss and gain of the respective energy components due to horizontal and vertical mixing, e.g., S_{K_M} includes the production of mean kinetic energy due to wind work at the surface and dissipation due to bottom friction. For further details, the reader is referred to *Fossum and Røed* (2006) or *Røed* (2006). Of particular interest are the two reversible energy exchange terms, C_{ME} and C_E^Φ, that allows the eddy kinetic energy to increase at the expense of the mean kinetic and average potential energy, respectively (Figure 2). The depth integrated conversion between mean and eddy kinetic energy contains two terms,

$$C_{ME} = -\rho_0 \int_{-1}^{0} (\overline{D\mathbf{u}'\mathbf{u}'} \cdot \nabla_\sigma \cdot \hat{\mathbf{u}} + \overline{\omega \mathbf{u}'} \cdot \partial_\sigma \hat{\mathbf{u}}) d\sigma, \tag{4}$$

where, $\hat{\mathbf{u}}$ is the mean motion[1], $\mathbf{u}'$ is the eddy motion, and ω is the vertical velocity relative to the σ-surfaces. The first is due to the horizontal shear in the mean current and its contribution is hence the familiar horizontal shear instability. The second is due to the vertical shear, and thus is the vertical shear instability (Kelvin-Helmholtz).

[1]Note that the mean current, $\hat{\mathbf{u}}$, is defined as, $\hat{\mathbf{u}} = \overline{D\mathbf{u}}/\overline{D}$, where the bar denotes a simple space-time average, and $\overline{D}$ is the average thickness of the water column as detailed in *Fossum and Røed* (2006).

The depth integrated conversion between average potential and the eddy kinetic energy is,

$$C_E^\Phi = -\rho_0 g \int_{-1}^{0} (C_{E1}^\Phi + C_{E2}^\Phi + C_{E3}^\Phi) d\sigma. \tag{5}$$

The first two terms are associated with instability processes and are

$$C_{E1}^\Phi = \overline{D''D\mathbf{u}'} \cdot (\int_\sigma^0 \nabla_\sigma \hat{\epsilon} d\sigma'), \qquad C_{E2}^\Phi = \overline{D\epsilon'\mathbf{u}'} \cdot \nabla_\sigma (\overline{D}\sigma + \overline{\eta}). \tag{6}$$

Here g is the gravitational acceleration, $\epsilon = (\rho - \rho_0)/\rho_0$ the density deviation and ρ the density. The mean density deviation, $\hat{\epsilon}$, like the mean motion is defined as a depth weighted average, that is, $\hat{\epsilon} = \overline{D\epsilon}/\overline{D}$. The fluctuating density deviation is denoted ϵ', and D'' and is the thickness deviation from its mean. Similarly are $\overline{\eta}$ and η'' the mean and fluctuating sea surface deviation, respectively. The remaining term is

$$C_{E3}^\Phi = \overline{D\mathbf{u}' \cdot \nabla_\sigma \eta''} + \overline{D\mathbf{u}' \cdot \nabla_\sigma \left[\int_\sigma^0 (D''\hat{\epsilon} + D\epsilon') d\sigma' \right]} + \overline{D\epsilon \mathbf{u}' \cdot \nabla_\sigma (D''\sigma + \eta'')}, \tag{7}$$

which is associated with conversions from eddy potential to eddy kinetic energy.

Negative values of C_{ME} indicate a transfer of energy from the mean kinetic energy directly to the eddy kinetic energy and is associated with barotropic instability. Positive values of C_E^Φ indicate a transfer of energy from average potential energy to the eddy kinetic energy and is normally associated with baroclinic instability. As noted in the previous paragraph, not all the terms that contributes to an energy conversion are interpretable as instabilities. An instability is normally defined as exponential growth of perturbations on the expense of the mean motion (in particular the gradients). Thus while the contributions in (6) represent such processes the contributions contained in (7) do not. Finally it should be mentioned that it is not straightforward to give a meaningful definition of what is meant by mean and eddy motion in a realistic setting. Here, we follow *Røed and Fossum* (2004) using a 25 hour block average to filter out the higher frequency motion, such as diurnal and semi-diurnal tides, from the remaining motion. Similar to *Røed and Fossum* (2004) and *Fossum* (2006) a 30 day time average is used to define the mean motion.

3.2. **Potential vorticity.** The development of the PV analysis tool is based on the works of *Charney and Stern* (1962), *Kushner* (1995) and *Ripa* (1991). The Charney-Stern criterion states that a necessary condition for a jet to become unstable is that the gradient of Ertel's PV vanish across the a jet. Thus to monitor areas susceptible to instability, it is sufficient to monitor extremes of Ertel's PV. Utilizing the transformation equations in *Griffies* (2004) Ertel's PV in σ-coordinates is

$$\mathcal{Q} = -\frac{1}{\rho_0 D} \left[(\tilde{\zeta} + f) \partial_\sigma \sigma_\theta + \mathbf{k} \cdot (\partial_\sigma \mathbf{u} \times \nabla_\sigma \sigma_\theta) \right]. \tag{8}$$

Here the σ-coordinate rendition of the relative vorticity is given by $\tilde{\zeta} = \mathbf{k} \cdot \nabla_\sigma \times \mathbf{u}$, f is the Coriolis parameter and σ_θ is the potential density. Furthermore, to arrive at (8) it is assumed that the horizontal scale is small enough for the horizontal component of the Earth's rotation to safely be neglected, and the hydrostatic and Boussinesq approximations are applied.

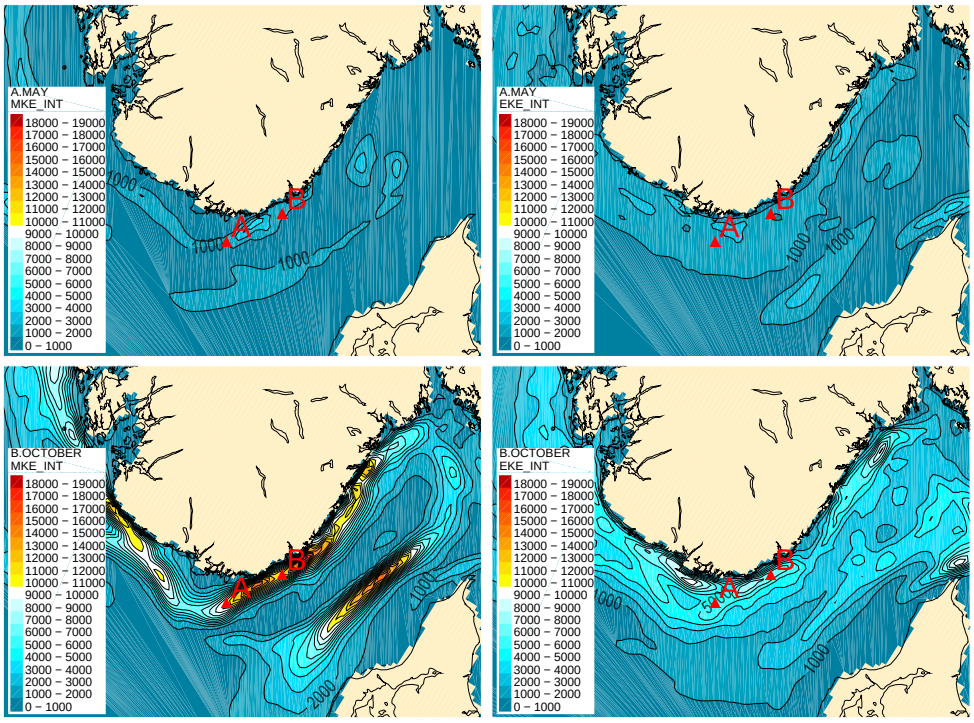

FIGURE 3. K_M (left-hand panels) and K_E (right-hand panels) for May (upper panels) and October (lower panels). Contour interval is 1000 J/m^2. In both months K_M reflects the mean current pattern in Skagerrak. The maximum in K_M off the Danish coast corresponds to the relatively strong inflow of Atlantic water along the coast toward northeast, and the maximum in K_M along the southeastern coast of Norway mirrors the relatively large mean currents in the NCC toward southeast. Note that October is a much more energetic month than May.

4. DISCUSSIONS AND CONCLUDING REMARKS

We have simulated the years 1997, 1998 and 2000-2003. Although there are year to year variations the kinetic energy pattern, as illustrated in Figure 3, are very similar and exhibits the same seasonal dependence. Notably the eddy kinetic energy is generally larger than the mean kinetic energy off the southern tip of Norway. This underscores that this region is an area of high variability, and is consistent with the anticyclonic eddies frequently observed here. Figure 3 also reveals that the NCC veers offshore just before the eddy region. Both C_{ME} and C_E^{Φ} are maximum close to the position where the NCC veers offshore (at the points marked A and B in Figure 3), and that C_{ME} dominates. This implies that both baroclinic and barotropic instability mechanisms are active, but that the barotropic dominates. The instability is confirmed by the PV analysis. The conversion terms also have extremes at approximately the same locations throughout the whole year. This suggests that the eddies should always appear at the same location, a fact confirmed by satellite observations (not shown).

The above leads us to conclude that a combination of baroclinic and barotropic instabilities located where the NCC veers offshore are responsible for the generation of anticyclonic eddies off the southern tip of Norway. Detailed analysis of the various contributions reveals that the vertical shear instability dominates, that is, the second term of (4). The seasonal variation of the instability and correspondingly the eddy kinetic energy is large (Figure 3), with strongest instability in the autumn and winter, when the wind energy input is large and increases the vertical shear. In addition as shown by *Fossum* (2006), in accord with the findings of *Aure and Sætre* (1981), a sudden outbreak of low salinity water may occur when the wind conditions change after a period of westerly winds have blocked the Skagerrak outflow. This will tend to increase not only the horisontal density gradients, but also the vertical shear through the thermal wind balance. This offers a simple physical explanation why there is a connection between the outbreak events and the observed eddies, as suggested by *Furnes et al.* (2001) and *Melsom* (2005).

It remains to explain why the NCC veers offshore. This is the same as asking why the instability seem to occur at the same place throughout the whole simulation period. Two suggestions were offered by *Røed and Fossum* (2004). The first is vortex squeezing and the second is a separation in a hydraulic sense due to the large coastline curvature (*Røed*, 1980). The latter may be investigated by using one of the criteria of *Klinger* (1994). As shown by *Fossum* (2006) it is not realistic for the NCC to separate hydraulically from the coast. Regarding the second it was concluded by *Fossum* (2006) that when the fluid is statically stable ($\frac{\partial \rho}{\partial z} < 0$), the above expression is always positive, and thus favors offshore veering.

Acknowledgments. This research was supported by the Research Council of Norway (NFR) through Project Nos. 140264/120 and 143559/431.

References

Albretsen, J. (2006), Impact of freshwater effluence on the circulation in the Skagerrak/northern North Sea Part II: Energy analysis, *in prep.*

Albretsen, J., and L. P. Røed (2006a), Sensitivity of Skagerrak dynamics to freshwater discharges: insight from a numerical model, in *European Operational Oceanography: Present and Future*, edited by H. Dahlin and P. Ryder, to appear in the Proceedings from the 4th EuroGOOS Conference, 6-9 June 2005, Brest France.

Albretsen, J., and L. P. Røed (2006b), Impact of freshwater effluence on the circulation in the Skagerrak/northern North Sea Part I: Model validation, *in prep.*

Aure, J., and R. Sætre (1981), Wind effects on the Skagerrak outflow, in *The Norwegian Coastal Current. Proceedings Norwegian Coastal Current Symposium, Geilo 9-12 Sept. 1980*, edited by R. Sætre and J. Aure, pp. 263–293, Univ. Bergen, Bergen, Norway.

Charney, J. G., and M. E. Stern (1962), On the stability of internal baroclinic jets in a rotating atmosphere, *J. Atmos. Sci.*, *19*, 159–172.

Danielssen, D. S., L. Edler, S. Fonselius, L. Hernroth, M. Ostrowski, and E. Svendsen (1997), Oceanographic variability in Skagerrak/northern Kattegat, May-June 1990., *ICEC J. Mar. Sci.*, *55*, 753–773.

Fossum, I. (2006), Analysis of instabilities and mesoscale motion off southern Norway, *J. Geophys. Res., in press.*

Fossum, I., and L. P. Røed (2006), Analysis of instabilities and mesoscale motion in continuously stratified ocean models, *J. Mar. Res., in press*.

Furnes, G., H. Engedahl, D. Hareide, and J. Aure (2001), Ocean eddies along the coast of southern Norway: Looking back on the 18 november 2000 event at the troll field. (in Norwegian, original title: Strømvirvler langs kysten av Sør-Norge: Et tilbakeblikk på hendelsen på Trollfeltet 18. november 2000.), *Tech. Rep. ID NH-00039406*, Norsk Hydro Sandvika, Norway.

Griffies, S. M. (2004), *Fundamentals of ocean climate models*, Princeton University Press.

Klinger, B. (1994), Inviscid current separation from rounded capes, *J. Phys. Oceanogr.*, *24*, 1805–1811.

Kushner, P. (1995), A generalized Charney-Stern theorem for semi-geostrophic dynamics, *Tellus*, *47*, 541–547.

LaCasce, J., and H. Engedahl (2005), Statistics of low frequency currents over the western Norwegian shelf and slope II: Model, *Ocean Dyn.*, *55*, 222–237, doi 10.1007/s10,236–005–0022–5.

Melsom, A. (2005), Mesoscale activity in the North Sea as seen in ensemble simulations, *Ocean Dyn.*, *55*, 338–350, doi 10.1007/s10,236–005–0016–3.

Ripa, P. (1991), General stability conditions for a multi-layer model, *J. Fluid Mech.*, *222*, 119–137.

Rodhe, J. (1987), The large-scale circulation in the Skagerrak, interpretation of some observations., *Tellus*, *39A*, 245–253.

Røed, L. P. (1980), Curvature effects on hydraulically driven inertial currents, *J. Fluid Mech.*, *96*, 395–412.

Røed, L. P. (1999), A pointwise energy diagnostic scheme for multilayer, nonisopycnic, primitive equation ocean models, *Mon. Weath. Rev.*, *127*, 1897–1911.

Røed, L. P. (2006), A pointwise energy diagnostic scheme for eddy resolving coastal ocean models, *Ocean Modeling, in revision*.

Røed, L. P., and I. Fossum (2004), Mean and eddy motion in the Skagerrak/northern North Sea: insight from a numerical model, *Ocean Dynamics*, *54*, 197–220.

Sætre, R., and M. Mork (Eds.) (1981), *The Norwegian Coastal Current. Proceedings from the Norwegian Coastal Current Symposium, Geilo 9-12 September 1980*, University of Bergen, Bergen, Norway.

Skogen, M. D., E. Svendsen, and H. Søiland (2002), Environmental status of the Skagerrak and North Sea 2000, *Tech. rep.*, Institute of Marine Research, Bergen, Norway, Available at http://www.imr.no/ morten/nocomments.

Skogen, M. D., E. Svendsen, and H. Søiland (2003), Environmental status of the Skagerrak and North Sea 2001, *Tech. rep.*, Institute of Marine Research, Bergen, Norway, Available at http://www.imr.no/ morten/nocomments.

Svansson, A. (1975), Physical and chemical oceanography of the Skagerrak and the Kattegat, 1. Open sea conditions., *Tech. Rep. 1*, Fishery Board of Sweden, Marine Research Institute.